

# Computer study of the structure and thermal stability of a monolayer MoS<sub>2</sub> film on a diamond substrate

A. Y. Galashev<sup>†,1,2</sup>, K. A. Ivanichkina<sup>1</sup>

<sup>†</sup>alexander-galashev@yandex.ru

<sup>1</sup>Institute of High-Temperature Electrochemistry of the UB RAS, 20 Akademicheskaya St., Yekaterinburg, 620990, Russia

<sup>2</sup>Ural Federal University n. a. the first President of Russia B. N. Yeltsin, 19 Mira St., Yekaterinburg, 620002, Russia

MoS<sub>2</sub> is a promising candidate for next-generation electrical and optoelectronic devices. The use of chemical vapor deposition allows obtaining high-quality MoS<sub>2</sub> monolayers on a diamond substrate. However, it is not clear how firmly the MoS<sub>2</sub> monolayer is held on the diamond substrate at a high temperature and how the structure of the MoS<sub>2</sub> monolayer changes after its deposition on the diamond substrate and subsequent heating on it. In this paper, the molecular dynamics method is used to study the stability of single-layer MoS<sub>2</sub> in the temperature range of 250 – 550 K. The molybdenum disulfide film on a diamond substrate structure is studied by constructing Voronoi polyhedra. Polyhedra were built around Mo atoms, and faces are formed by neighboring S atoms. The distributions of polyhedrons by the number of faces were found. These distributions were also calculated for truncated polyhedra obtained by eliminating small geometric elements. A comparison of the obtained statistical distributions for a MoS<sub>2</sub> monolayer on a diamond substrate with the corresponding characteristics of an autonomous monolayer MoS<sub>2</sub> indicates a significant change in the structure of the monolayer. This change is a result of its deposition on the diamond substrate. When the temperature reaches 550 K, the MoS<sub>2</sub> film is completely separated from the substrate. There is a singularity near this temperature, which indicates the thermal instability of the system under investigation.

**Keywords:** diamond, molecular dynamics, molybdenum disulfide, stability.

УДК: 544.032: 53.096

# Компьютерное изучение структуры и термической устойчивости однослойной пленки MoS<sub>2</sub> на алмазной подложке

Галашев А. Е.<sup>†,1,2</sup>, Иваничкина К. А.<sup>1</sup>

<sup>1</sup>Институт высокотемпературной электрохимии, УрО РАН, ул. Академическая, 20, Екатеринбург, 620990, Россия

<sup>2</sup>Уральский федеральный университет им. первого президента России Б. Н. Ельцина, ул. Мира, 19, Екатеринбург, 620002, Россия

MoS<sub>2</sub> является перспективным материалом для создания на его основе устройств в отраслях электроники и оптоэлектроники. Использование метода химического осаждения из газовой фазы позволяет получать высококачественные однослойные пленки MoS<sub>2</sub> на алмазной подложке. Однако, остаются открытыми вопросы касающиеся прочности сцепления MoS<sub>2</sub> с подложкой при высокой температуре, а также особенностей структурных изменений MoS<sub>2</sub> после его осаждения на подложку и последующем росте температуры. В настоящей работе методом молекулярной динамики была исследована устойчивость однослойного MoS<sub>2</sub> в диапазоне температур 250 – 550 К. Структура пленки дисульфида молибдена на алмазной подложке изучалась методом построения многогранников Вороного. Многогранники строились с центром в атомах молибдена так, что соседние атомы серы образовывали грани. Найдены распределения многогранников по числу граней. Эти распределения были также рассчитаны для усеченных многогранников, полученных методом исключения малых геометрических элементов. Сравнение полученных статистических распределений для монослоя MoS<sub>2</sub> на алмазной подложке с соответствующими характеристиками автономного MoS<sub>2</sub> указывает на значительное изменение структуры монослоя. Это изменение является результатом осаждения дисульфида молибдена на алмазную подложку. В случае достижения системой температуры в 550 К пленка полностью отделяется от подложки. При данной температуре исследуемая система становится термически не устойчива.

**Ключевые слова:** алмаз, молекулярная динамика, дисульфид молибдена, устойчивость.

## 1. Introduction

Molybdenum disulfide ( $\text{MoS}_2$ ) is a semiconductor with a bulk band gap above 1.2 eV [1], which can be further modified by changing its thickness [2]. The change in the band structure with the layer number is due to quantum confinement and the resulting change in hybridization between  $p_z$  orbitals of sulfur atoms and  $d$ -orbitals on Mo atoms. This final band gap is the key cause of excitation around  $\text{MoS}_2$  compared to graphene, since graphene has a zero band gap unless strain [3] or other gap-opening engineering is performed [4]. Because of its direct band gap, as well as its well-known properties as a lubricant,  $\text{MoS}_2$  has attracted considerable attention lately [5,6]. The atomic-level mechanism for the growth of  $\text{MoS}_2$  phases by sulfidation of  $\text{MoO}_3$  crystals was identified in [7]. Porous carbon and carbon nanotubes can be used as electrodes of lithium-ion batteries (LIB) and supercapacitors, especially in combination with organic electrolytes [8,9]. The use of  $\text{MoS}_2$  as an anode for LIB will significantly increase the capacity of batteries [10].

Monolayer  $\text{MoS}_2$  has not only a direct band gap ( $\sim 1.8$  eV), but also a high mobility of carriers [11,12]. The electronic, optoelectronic, and mechanical properties of  $\text{MoS}_2$  nanosystems have been determined theoretically [12–14]. Experimentally, monolayer  $\text{MoS}_2$  transistors have been demonstrated, which show high performance, for example, mobility of at least  $200 \text{ cm}^2 \text{ V}^{-1} \text{ S}^{-1}$  and on/off ratios at a room temperature of  $1 \times 10^8$  [12,13]. These studies show that monolayer  $\text{MoS}_2$  can be an ideal electronic and optoelectronic material. However, the thermal conductivity of  $\text{MoS}_2$  is much lower, which can cause problems with its thermal stability and limit the development of devices based on this nanomaterial [12,13].

Extremely high hardness and thermal conductivity, radiation and chemical resistance, optical and electrical characteristics, as well as a number of other parameters make the diamond very promising for use in traditional and developing electronic technologies. Monolayer  $\text{MoS}_2$  on a diamond substrate can be used to fabricate a field effect transistor (FET). Diamond films on silicon having an average crystallite size of  $\sim 1 \mu\text{m}$  can be obtained by thermal gas-phase deposition [15]. Diamond has a band gap  $\sim 6$  eV [16]. The energy of formation of an electron-hole pair in diamond is very large ( $\sim 10$  eV), which is 2.8 times higher than in silicon. Estimates give a value of  $1800 - 2200 \text{ cm}^2 \text{ V}^{-1} \text{ S}^{-1}$  for the mobility of electrons in diamond, which is noticeably higher than in silicon ( $1500 \text{ cm}^2 \text{ V}^{-1} \text{ S}^{-1}$ ). On a diamond substrate, films of various two-dimensional materials can be grown. The main purpose of  $\text{MoS}_2$  on diamond wafers can be its use in thermal-management schemes for high-power semiconductor devices. Since diamond transports heat equally well in all three dimensions, it can act as an excellent heat spreader.  $\text{MoS}_2$  on diamond plates should dramatically reduce thermal resistance and, in turn, the gate temperature of semiconductor devices, leading to a higher power density.

The aim of this work is to study the structure and thermal stability of a monolayer  $\text{MoS}_2$  film on a diamond substrate in the temperature range  $250 \leq T \leq 550 \text{ K}$ .

## 2. Computer model

Using the LAMMPS program, calculations at each temperature were performed by the classical molecular dynamics [17]. A key element of molecular dynamics modeling is the selection of an appropriate empirical potential. In this paper, to describe the interaction of Mo and S atoms in the structure of  $\text{MoS}_2$ , the many-body potential of the Stillinger-Weber type is used [18]. The weak van der Waals interaction of molybdenum disulfide and the substrate was described by the Morse potential, which decreases rapidly with distance [19]. The C atoms of the diamond substrate were immovable. Therefore, the interactions of C-C were not taken into account, which was justified, because the interaction between the substrate and the  $\text{MoS}_2$  film was weak. This significantly reduced the calculation time without affecting the simulation result.

The simulation was performed in the following order. At the beginning of the simulation, a  $\text{MoS}_2$  layer, measuring  $3.79 \times 4.1 \text{ nm}$ , was located on a diamond substrate at a distance of 0.351 nm. This distance is somewhat larger than the S-C distance (0.334 nm) between the plane of the S atom of the  $\text{MoS}_2$  film and the graphene sheet adjacent to it that was determined by *ab initio* calculations in [20]. The calculations were performed using a system of 2040 atoms (1440 C atoms, 400 S atoms, and 200 Mo atoms). The C atoms in these calculations remained immobile, but interacted with the Mo and S atoms. The fixation of the C atoms of the substrate should not have a large effect on the simulation result. The highest of the temperatures we considered was only 11% of the diamond “melting” temperature. In fact, heating up diamonds under the pressure of 0.1 MPa turns them into graphite first. Only further heating would cause “melting”. “Liquid diamond” could be achieved under the pressure of about 10 GPa and temperature of 5000 K. Therefore, thermal vibrations of diamond atoms even at  $T = 550 \text{ K}$  can be neglected. This conclusion is also confirmed by the fact that the bonds between carbon atoms in diamond are much stronger than the bonds between the Mo-Mo, S-S or Mo-S atoms. Such an approximation has already been used by us in models adequately representing the migration of  $\text{Li}^+$  ions through graphene membranes with holes [21,22], also in the simulation of silicene on pyrolytic graphite [23]. In addition, this carbon substrate can be considered as part of an infinitely large flat C system, without resorting to periodic boundary conditions (PBC). The boundary conditions used make it possible to observe the behavior of the edges of the film on the substrate when the temperature changes. In the present model, the diamond substrate was turned to a  $\text{MoS}_2$  film by the (001) plane. The time step  $\Delta t$  was 0.1 fs. This is a typical time step used to model low-dimensional systems with a complex interaction of atoms of various types [24–26]. The use of a larger time step leads to an increase in temperature during the calculation.

In 10 ps ( $100000 \Delta t$ ), the system relaxed to a state with a predetermined temperature reaching the minimum value of internal energy. Further, the temperature was raised to the required temperature (from 250 K to 550 K) for 40 ps. Then, the system was in the state under the conditions of

the NPT ensemble (at  $P=0.1$  MPa) created by the Nose — Hoover barostat for 100 ps. The temperature dependence of enthalpy was determined in molecular dynamic calculations in the NPT ensemble. The isobaric heat capacity as a function of temperature  $c_p(T)$  was calculated by numerical differentiation of this dependence. The calculations were performed both for an autonomous monolayer of  $\text{MoS}_2$  and for  $\text{MoS}_2$  on a diamond substrate. Eight processors were used in calculations that were performed on the “Uran” cluster at the Institute of Mathematics and Mechanics of the Ural Branch of the Russian Academy of Sciences. The duration of all calculations was 35 hours.

Structural analysis of small objects can be carried out using the statistical geometry method, based on the construction of the Voronoi polyhedra (VPs) [27]. In the case of a polyatomic system, atoms of one type may play the role of polyhedron centers, while atoms of another type may serve as their nearest neighbors, determining the polyhedron faces [28]. For example, in the case of the  $\text{MoS}_2$  system, it is advantageous to use molybdenum atoms as the centers and select the nearest neighbors among the S atoms. These hybrid polyhedra are easier to construct since the number of S atoms is twice that of the Mo ones. However, in the case where different sizes of atoms are used, the hybrid polyhedra are not Voronoi polyhedra, since they fail to fill completely all of the space occupied by molecules without voids and overlaps.

The VP faces determine the cyclic structures formed from Mo atoms, while hybrid polyhedron faces determine rings composed of S atoms. However, there is another way to construct the VPs in a multicomponent system when the sizes of all atoms are the same. Here we will not take into account the difference in the sizes of Mo and S atoms in the VP construction, and we will construct VP for Mo atoms when the geometric neighbors are only S atoms. The polyhedra were constructed through every 1000 time steps around 162 Mo atoms. Mo atoms forming the edges of the sheet did not participate in the construction of polyhedra. The absence of boundary atoms among the centers of polyhedra avoids a situation when there is not a single atom S in the half-space considered for Mo atom. In this case, the polyhedron can be constructed in the presence of four or more neighboring S atoms, that is, under the condition realized in the model.

A sufficient condition for the thermal stability of a homogeneous system with respect to small changes in thermodynamic parameters with constant thermodynamic forces is defined as [29]

$$\frac{T}{c_p} > 0, \quad (1)$$

where  $c_p$  is the isobaric heat capacity.

Mean distance between the  $\text{MoS}_2$  monolayer and the diamond substrate was calculated as

$$h_g = \frac{1}{N} \sum_{i=1}^N r_{S_i-C}^{\min} \quad (2)$$

where  $N$  is the number of C atoms on the lower surface of the  $\text{MoS}_2$  monolayer,  $r_{S_i-C}^{\min}$  is the minimum distance between the  $i$  atom S of the lower surface of the  $\text{MoS}_2$  monolayer and the surface of the diamond substrate.

The cohesive energy between the mono-layer  $\text{MoS}_2$  film and the graphite substrate was calculated by the formula:

$$E_{coh} = E_{\text{MoS}_2} + E_C - E_{\text{C+MoS}_2}, \quad (3)$$

where  $E_{\text{C+MoS}_2}$ ,  $E_{\text{MoS}_2}$ , and  $E_C$  are the total energies obtained, as a result, of calculations for two-dimensional molybdenum sulfide on a graphite substrate,  $\text{MoS}_2$  and a substrate, respectively.

### 3. Results

The  $\text{MoS}_2$  configuration on a diamond substrate, obtained at a time of 100 ps in a MD calculation at  $T=550$  K using an NPT ensemble, is shown in Fig. 1. It is seen that the  $\text{MoS}_2$  film turned out to be quite far from the substrate. In other words, the substrate practically lost its supporting function, and the film actually became autonomous. No significant damage to the film at this instance can be traced; the film retains its crystalline structure. However, the surface of the film (especially the lower one facing the substrate) is no longer ideally flat, although the vertical deviation of the extreme S atoms in the film from the mean  $z$ -coordinate of the entire film is not large ( $<4\%$ ).

The monolithicity and structural distortions of the film were verified using the method of statistical geometry, which is very sensitive to changes in the local order in the arrangement of atoms. In this case, this method was based on the construction of hybrid polyhedra. All the statistical distributions of the polyhedron elements obtained in the temperature interval turned out to be similar.

The Mo atoms in our system with substrate have a wide  $n$ -spectrum of geometric neighbors (Fig. 2 a), which is primarily due to the almost flat arrangement of S atoms in the upper and lower planes adjacent to the plane of the metal atoms. The maximum of this distribution is at  $n=25$ . Consequently, approximately twelve S atoms in each of the planes are most often the nearest neighbors of the Mo atom. Most of these neighbors do not have a strong Mo-S bond.

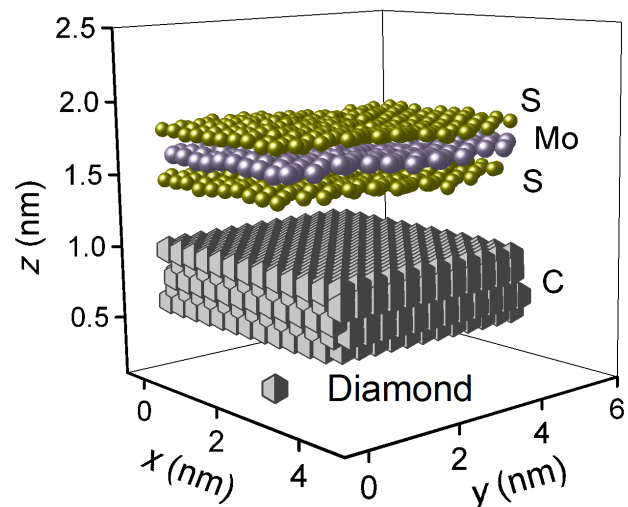


**Fig. 1.** A monolayer  $\text{MoS}_2$  film on a diamond substrate at the time moment of 100 ps and a temperature of 550 K. The distance between the  $\text{MoS}_2$  film and the diamond substrate is 0.41 nm.

The  $n$ -spectrum of autonomous  $\text{MoS}_2$  is significantly different from the corresponding  $\text{MoS}_2$  spectrum on the substrate, in particular, the distribution maximum is shifted by  $n=18$ .

True polyhedra give a wide  $n$ -distribution (according to the number of faces), while for truncated polyhedrons this distribution is narrower and shifted to the left (Fig. 2b). Note that in either case, the  $n$ -distribution for autonomous  $\text{MoS}_2$  differs markedly from the corresponding distribution for a  $\text{MoS}_2$  monolayer on a diamond substrate. The character of the intensities in the  $n$ -distributions of the polyhedra of the autonomous  $\text{MoS}_2$  varies, but the width of the spectra is unchanged.

During the simulation, the monolayer  $\text{MoS}_2$  was peeled off from the substrate material (Fig. 3). If the distance  $h_g$  between  $\text{MoS}_2$  and the substrate material was 0.351 nm at  $T=250$  K, then at 350 K it increased by 0.03 nm, and at a temperature of 550 K it was 0.41 nm. An increase in temperature is accompanied not only by an increase in the distance from the film to the substrate but also by a reduction in the binding energy between them. The cohesive energy  $E_{coh}$  between the  $\text{MoS}_2$  film and the substrate increases with temperature. This increase amounted to 0.68 eV with a temperature change from 250 K to 550 K (Fig. 3).

Both dependences in Fig. 3 show significant growth at  $T > 500$  K. In order to understand the cause for these changes, we calculated heat capacity  $c_p$  as  $(\partial H / \partial T)_p$  of the “ $\text{MoS}_2$ -diamond substrate” system for each of the temperatures considered here.

To compare the calculated enthalpy of  $\text{MoS}_2$  with the experimental value, we determined its difference  $\Delta H$  from the formation enthalpy at the reference temperature of 298.15 K. The  $\Delta H$  value obtained by us was  $-264 \pm 22$  kJ/mol, whereas this value for such a real system was  $-285$  kJ/mol [30].

The temperature dependence of the criterion for the thermal stability  $T/c_p$  of the  $\text{MoS}_2$  film on a diamond substrate is shown in Fig. 4. Deformation of the  $\text{MoS}_2$  film is due to the inherent lattice mismatch of the diamond and molybdenum disulfide. The gap between the film and the surface increases with increasing temperature. At a certain temperature  $T^* = 550$  K, the heterostructure loses stability due to the detachment of the Si film from the diamond surface.

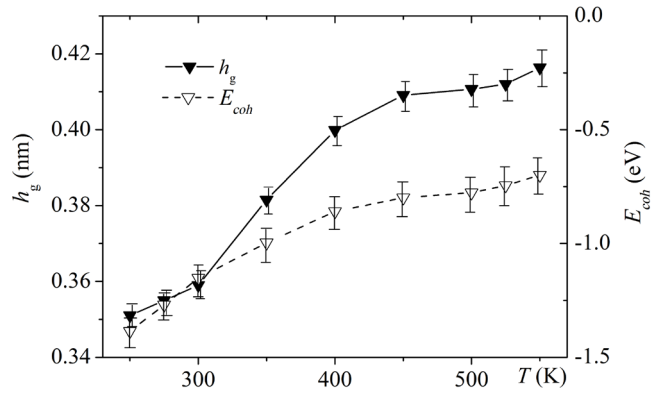


**Fig. 3.** Temperature dependence of mean distance and cohesion energy between  $\text{MoS}_2$  and substrate; statistical errors in simulations are shown in error bars.

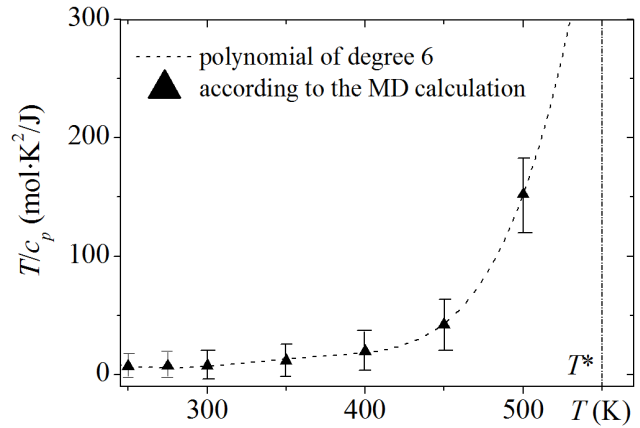


**Fig. 4.** Temperature dependence of the isodynamic thermal stability coefficient;  $T^*$  is the temperature loss of thermal stability.

#### 4. Discussion

Thin-layer  $\text{MoS}_2$  is well suited as a channel material in field-effect transistor applications [12,13]. It exhibits high mobility, almost ideal switching characteristics and low standby power dissipation. The mobility of the  $\text{MoS}_2$  FETs could be significantly improved by using  $\text{HfO}_2$ , as gate materials. Recently developed field-effect SiC transistors can function fairly stably at 723 K for 600 hours [31]. According

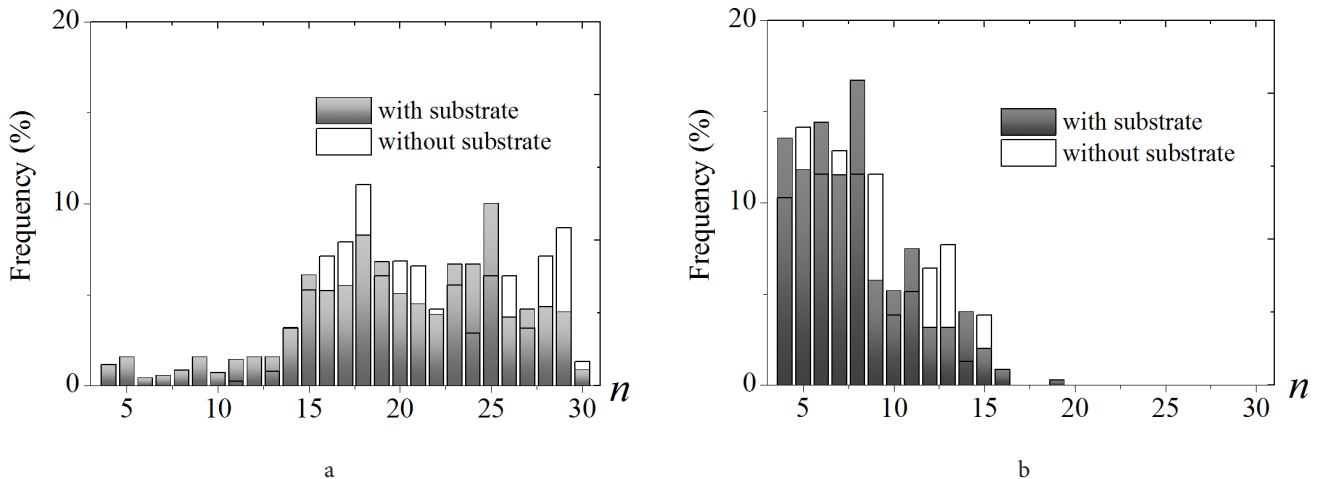


**Fig. 2.** Distribution of hybrid polyhedra by the number of faces in an autonomous  $\text{MoS}_2$  film and that on a diamond substrate at a temperature of 550 K: (a) true polyhedra, (b) truncated polyhedra.



to the data obtained by us the “MoS<sub>2</sub>-diamond” field-effect transistor can operate only at temperatures lower than 550 K. The gap  $h_g$  between the MoS<sub>2</sub> film and the diamond substrate is the most pronounced change with increasing temperature. This value increases by 19% when the temperature changes from 250 K to 550 K.

Even at the lowest temperature (250 K) the MoS<sub>2</sub> film took on a wave form. As the temperature increased over the middle of the substrate, a “hump” or “troughs” of the film could be found, but at 550 K the film was substantially straightened, so that its wave-like profile was almost invisible.

The isobaric specific heat for monolayer MoS<sub>2</sub> on diamond, calculated within the framework of the NPT ensemble, has a maximum of 300 K. A distinctive feature of the consideration of the specific heat of the film is that in the enthalpy it is necessary to include not only the enthalpy of the volume phase, but also the surface enthalpy introduced in due time by Guggenheim [32]

$$H = H_b + H_s \quad (4)$$

Since the pressure  $p$  does not belong to the parameters of the nonautonomous surface phase, the surface enthalpy coincides with the excess surface energy

$$H_s = u_s \cdot S, \quad (5)$$

here  $u_s$  is the specific total surface energy,  $S$  is the surface area of the film. Taking into account (3) and (4), the expression for the specific heat can be written in the form

$$c_p = c_p^{(b)} + c_p^{(s)} = c_p^{(b)} + \frac{\partial(u_s S)}{\partial T}, \quad (6)$$

where  $c_p^{(b)}$  is the volume part of the specific heat,  $c_p^{(b)} > 0$ .

The area of the entire surface can be expressed in terms of the number  $N$  of atoms and the density  $\rho$  of atoms

$$S = 2 \cdot L_x \cdot L_y + 2(L_x + L_y) \cdot L_z \approx 2N / (\rho \cdot L_z), \quad (7)$$

where  $L_z$  is the thickness of the film, which varies more slightly with an increase in temperature than the horizontal dimensions  $L_x$  and  $L_y$  of the film. Therefore, the lateral surface of the film is neglected.

Expressions for the surface enthalpy and its temperature derivative are written as follows:

$$H_s = 2u_s N / (\rho \cdot L_z), \quad (8)$$

$$\frac{\partial H_s}{\partial T} = 2 \frac{\partial u_s}{\partial T} \left[ \frac{N}{\rho \cdot L_z} \right] + \left\{ -2 \frac{\partial \rho}{\partial T} \left[ \frac{u_s N}{\rho^2 L_z} \right] \right\}. \quad (9)$$

The first term in expression (9) is negative and decreases with increasing the temperature much faster (more rapidly than linearly) than the positive second term (in curly brackets) increases [33]. Such a change in the derivative ( $\partial u_s / \partial T$ ) is associated with the formation of a wave-like profile of the film at high temperatures. The vertical displacement of atoms in the film sharply reduces its elasticity in the horizontal direction. The limit of thermodynamic stability is reached when the absolute values of the contributions ( $\partial H_b / \partial T$ ) and ( $\partial H_s / \partial T$ ) to the heat capacity become equal.

## 5. Conclusions

In this paper, we have considered the possibility of using a monolayer MoS<sub>2</sub> film on a diamond substrate in electronic devices, such as a field-effect transistor or a heat-generating gate junction. The detailed structure and thermal stability of such a film were studied in the temperature range of  $250 \leq T \leq 550$  K. We showed that the structure of a MoS<sub>2</sub> film on a diamond substrate differs from that of an MoS<sub>2</sub> autonomous monolayer. At the same time, the structure of the film on the substrate is not very sensitive to temperature changes. However, the thermal stability of the “MoS<sub>2</sub>-diamond substrate” system decreases with increasing temperature. This is due to a significant increase in the distance between the film and the substrate as the temperature rises. Finally, at a temperature of 550 K, the film completely separates from the substrate. Using a MoS<sub>2</sub> film on a diamond substrate at a temperature of 550 K and above can lead to the folding of the film and disrupting the operation of the electronic device.

## References

1. K. K. Kam, B. A. Parkinson. J. Phys. Chem. 86 (4), 463 (1982). [Crossref](#)
2. K. F. Mak, C. Lee, J. Hone, J. Shan, T. F. Heinz. Phys. Rev. Lett. 105, 136805 (2010). [Crossref](#)
3. V. M. Pereira, A. H. Castro Neto. Phys. Rev. Lett. 103, 046801 (2009). [Crossref](#)
4. K. S. Novoselov, A. K. Geim, S. V. Morozov, D. Jiang, M. I. Katsnelson, I. V. Grigorieva, S. V. Dubonos, A. A. Firsov. Nature. 438, 197 (2005). [Crossref](#)
5. Q. H. Wang, K. Kalantar-Zadeh, A. Kis, J. N. Coleman, M. S. Strano. Nat. Nanotech. 7 (11), 699 (2012). [Crossref](#)
6. M. Chhowalla, H. S. Shin, G. Eda, L. Li, K. P. Loh, H. Zhang. Nat. Chem. 5 (4), 263 (2013). [Crossref](#)
7. S. Hong, A. Krishnamoorthy, P. Rajak, S. Tiwari, M. Misawa, F. Shimojo, R. K. Kalia, A. Nakano, P. Vashishta. Nano Lett. 17 (8), 4866 (2017). [Crossref](#)
8. K. Wang, S. Zhou, Y. Zhou, J. Ren, L. Li, Y. Lan. Int. J. Electrochem. Sci. 13, 10766 (2018). [Crossref](#)
9. K. Wang, J. Pang, L. Li, S. Zhou, Y. Li, T. Zhang. Front. Chem. Sci. Eng. 12(3), 376 (2018). [Crossref](#)
10. J. Xiao, D. Choi, L. Cosimbescu, P. Koech, J. Liu, J. P. Lemmon. Chem. Mater. 22 (16), 4522 (2010). [Crossref](#)
11. T. Cheiwchanamngij, W. R. Lambrecht. Phys. Rev. B. 85, 205302 (2012). [Crossref](#)
12. B. Radisavljevic, A. Radenovic, J. Brivio, V. Giacometti, A. Kis. Nat. Nanotech. 6, 147 (2011). [Crossref](#)
13. Z. Yin, H. Li, H. Li, L. Jiang, Y. Shi, Y. Sun, G. Lu, Q. Zhang, X. Chen, H. Zhang. ACS Nano. 6 (1), 74 (2012). [Crossref](#)
14. Q. Peng, S. De. Phys. Chem. Chem. Phys. 15, 19427 (2013). [Crossref](#)
15. S. A. Linnik, A. V. Gaydaychuk, E. Y. Baryshnikov. Mater. Today: Proceedings. 3S, 138 (2016). [Crossref](#)
16. J. H. Gong, S. X. Lin, W. Li, J. Gao. Appl. Mech. Mater. 229–231, 74 (2012). [Crossref](#)
17. S. J. Plimpton. Comp. Phys. 117, 1 (1995). [Crossref](#)
18. J.-W. Jiang, H.-S. Park, T. Rabczuk. J. Appl. Phys. 114, 064307 (2013). [Crossref](#)

19. P. Nicolini, T. Polcar. *Comp. Mater. Sci.* 115, 158 (2016). [Crossref](#)
20. Y. Jing, E.O. Ortiz-Quiles, C.R. Cabrera, Z. Chen, Z. Zhou. *Electrochim. Acta.* 147, 392 (2014). [Crossref](#)
21. A. E. Galashev, Yu. P. Zaikov. *Rus. J. Electrochem.* 51 (9), 867 (2015). [Crossref](#)
22. A. E. Galashev, O. R. Rakhmanova. *High Temp.* 54 (1), 11 (2016). [Crossref](#)
23. A. E. Galashev, K. A. Ivanichkina. *Rus. J. Phys. Chem. A.* 91 (12), 2448 (2017). [Crossref](#)
24. A. E. Galashev, O. R. Rakhmanova, O. A. Novruzova. *High Temp.* 49 (2), 193 (2011). [Crossref](#)
25. A. E. Galashev, O. R. Rakhmanova, O. A. Novruzova. *High Temp.* 49 (4), 528 (2011). [Crossref](#)
26. A. E. Galashev, O. R. Rakhmanova. *High Temp.* 53 (3), 374 (2014). [Crossref](#)
27. V. P. Skripov, A. E. Galashev. *Rus. Chem. Rev.* 52, 97 (1983). [Crossref](#)
28. O. A. Novruzova, O. R. Rakhmanova, A. E. Galashev. *Rus. J. Phys. Chem. A.* 81 (11), 1825 (2007). [Crossref](#)
29. V. K. Semenchenko. *Selected Chapters of Theoretical Physiki. Moscow, Prosveschenie* (1966) 396 p. (in Russian). [В.К. Семенченко. Избранные главы теоретической физики. Москва, Просвещение (1966) 396 с.]
30. O. Knacke, O. Kubashewski, K. Hesselman. *Thermochemical properties of inorganic substances*, 2nd. edn. Verlag, Springer (1991) 861 p. [Crossref](#)
31. P. G. Neudeck, D. J. Stry, L. Y. Chen, R. S. Okojie, G. M. Beheim, R. D. Meredith, T. L. Ferrier. *Mater. Sci. Forum.* 556–557, 831 (2007). [Crossref](#)
32. E. A. Guggenheim. *Modern thermodynamics by the methods of Willard Gibbs.* Methuen & Co., Great Britain (1933) 206 p.
33. J. J. Gafner, S. Gafner, I. Zamulin, L. Redel, V. M. Samsonov. *Phys. Solid State.* 55 (10), 2142 (2013).